Noise-aware dictionary-learning-based sparse representation framework for detection and removal of single and combined noises from ECG signal

Udit Satija ✉, *Barathram Ramkumar, M. Sabarimalai Manikandan*

School of Electrical Sciences, Indian Institute of Technology Bhubaneswar, Bhubaneswar, Odisha 751013, India
✉ *E-mail: us11@iitbbs.ac.in*

Published in Healthcare Technology Letters; Received on 20th September 2016; Revised on 27th November 2016; Accepted on 8th December 2016

Automatic electrocardiogram (ECG) signal enhancement has become a crucial pre-processing step in most ECG signal analysis applications. In this Letter, the authors propose an automated noise-aware dictionary learning-based generalised ECG signal enhancement framework which can automatically learn the dictionaries based on the ECG noise type for effective representation of ECG signal and noises, and can reduce the computational load of sparse representation-based ECG enhancement system. The proposed framework consists of noise detection and identification, noise-aware dictionary learning, sparse signal decomposition and reconstruction. The noise detection and identification is performed based on the moving average filter, first-order difference, and temporal features such as number of turning points, maximum absolute amplitude, zerocrossings, and autocorrelation features. The representation dictionary is learned based on the type of noise identified in the previous stage. The proposed framework is evaluated using noise-free and noisy ECG signals. Results demonstrate that the proposed method can significantly reduce computational load as compared with conventional dictionary learning-based ECG denoising approaches. Further, comparative results show that the method outperforms existing methods in automatically removing noises such as baseline wanders, power-line interference, muscle artefacts and their combinations without distorting the morphological content of local waves of ECG signal.

1. Introduction: Accurate and reliable measurements of clinical features of electrocardiogram (ECG) signal are most important for effective diagnosis of cardiovascular diseases. In practice, ECG signals are mostly corrupted with different kinds of noise and artefacts such as baseline wander (BW), power-line interference (PLI), and muscle artefacts (MA) under resting and ambulatory conditions [1–11]. The noises present in the ECG signal may mask the morphological features of the local waves such as P-wave, QRS complex, T-wave and U-wave and thus degrade diagnostic quality. Various ECG denoising methods were presented based on an adaptive enhancer using second-order statistics [1], a signal decomposition-based modified Bayesian framework [2], sequential averaging filter using Bayesian framework [3], adaptive filter and wavelet shrinkage [5], non-local wavelet transform (WT) filtering [4], marginalised particle extended Kalman filter with an automatic particle weighting strategy [6], empirical mode decomposition (EMD) [7]. The hybrid denoising model is presented for removal of additive Gaussian noise [8]. Most MA removal methods are based on EMD [9], nonlinear Bayesian filtering framework [10], WT [12], EMD and WT [12], and sparse signal representation on mixed dictionaries [11]. The BW is removed based on the digital high pass filters, low-order polynomials [13], EMD [14], WT [15], and nonlinear filter bank [16].

Although many noise removal methods were presented for removing the ECG noises [1–17], most methods lack in preserving the morphological content such as amplitude, duration, polarity, shape and spectra of the ECG signal. Further, different signal processing approaches are employed for removal of different kinds of noises from ECG signal. Unlike other transformation-based methods, the representation dictionary learning is performed using both time-localised and frequency-localised elementary waveforms for effective representation of ECG signal and noises such as BW, PLI, and MA. However, computational complexity of the sparse representation highly relies on the size of a representation dictionary. From our previous studies, it is noted that the MA can be effectively removed from the ECG signal using sparse signal decomposition on mixed dictionaries including the impulsive and sinusoidal elementary waveforms and QRS information [11]. Furthermore, it is observed that the computational load can be reduced by choosing suitable number of time- and frequency-localised elementary waveforms based on the type of noises added to an ECG signal. To the best of our knowledge, there is no generalised sparse representation-based ECG noise removal framework for automatically detecting and removing the single and combined noises from the ECG signal.

In this Letter, we propose a noise-aware dictionary learning-based generalised ECG signal enhancement framework which not only preserves the morphological content of the local waves such as P, QRS, T, and U of the ECG signal but also significantly reduces computational load when compared with conventional dictionary learning-based sparse representation methods and other filtering methods. The main contribution of this Letter is to investigate different kinds of mixed dictionaries for removal of ECG noises and finding the optimal size for each of the representation dictionary learned based on the temporal-spectral characteristics of ECG noises such as BW, PLI, and MA. Based on the decomposition results, we present noise suppression algorithms for removal of single and combined ECG noises. Evaluation results demonstrate that the noise-aware dictionary-learning approach can significantly reduce the computational load when compared with the conventional dictionary learning-based ECG denoising methods.

The remainder of this Letter is organised as follows: Section 2 presents an ECG signal enhancement based on sparse representation with noise-aware dictionary learning algorithm. In Section 3, signal quality assessment results and computational analysis are presented. Finally, the conclusions are drawn in Section 4.

2. Methods and materials: This section presents an automated noise-aware dictionary learning-based sparse representation framework for removal of single and combined ECG noises such as BW, PLI, and MA, which are time-localised and frequency-localised signals. The flowchart of the proposed framework is illustrated in Fig. 1, which consists of three major

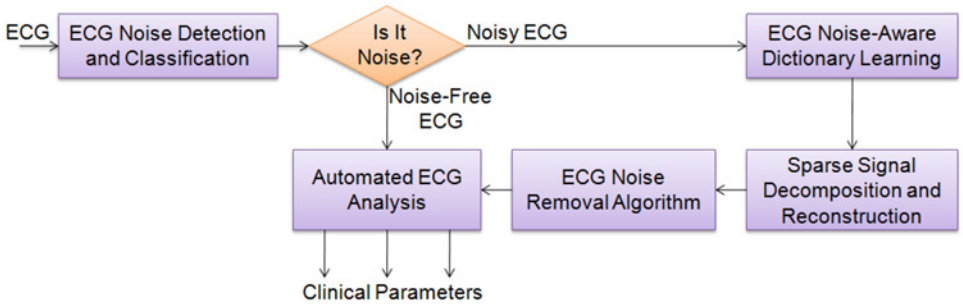

Fig. 1 *Proposed noise-aware dictionary-learning-based sparse representation framework for removal of single and combined ECG noises*

steps: noise detection and identification, noise-aware dictionary learning, and sparse representation-based noise removal algorithms. In the next-subsection, we describe each of the processing steps of the proposed framework.

2.1. Noise detection and identification: Many studies show that the accuracy and robustness of the quantitative parameter extraction system can be improved by incorporating a noise removal algorithm at the pre-processing step. Therefore, in this Letter, we attempt to present a generalised ECG enhancement framework which includes noise detection and identification, noise-aware dictionary learning, sparse signal decomposition and noise removal. The noise detection and identification is performed based on the moving average filter, the first-order difference, and the temporal features including maximum absolute amplitude (MAA), zerocrossings, and autocorrelation features (ACF). The

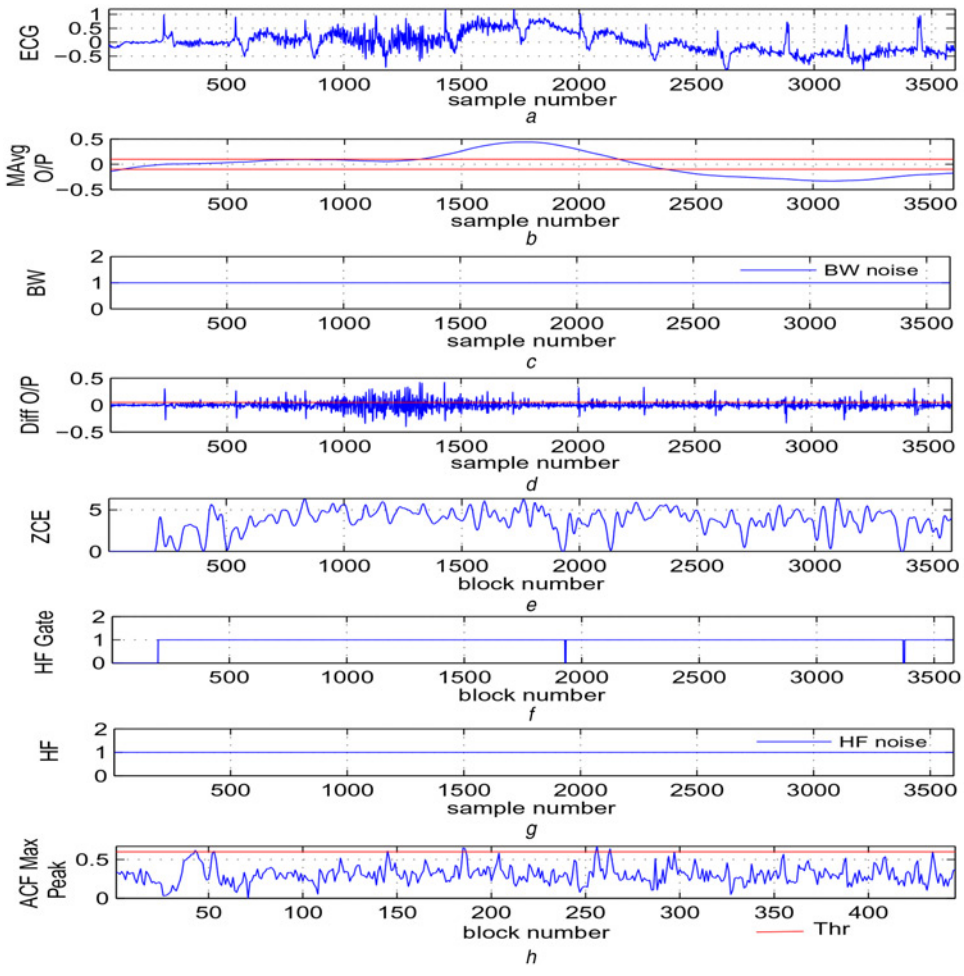

Fig. 2 *Noise detection and identification step*
a ECG corrupted with BW and MA taken from an MITBIHA record 104
b BW detection using MAA thresholding
c BW decision
d Difference operation output and MAA thresholding
e ZC envelope for detection of MA/PLI
f ZC thresholding for detection of MA
g MA decision
h ACF feature thresholding for detection of PLI

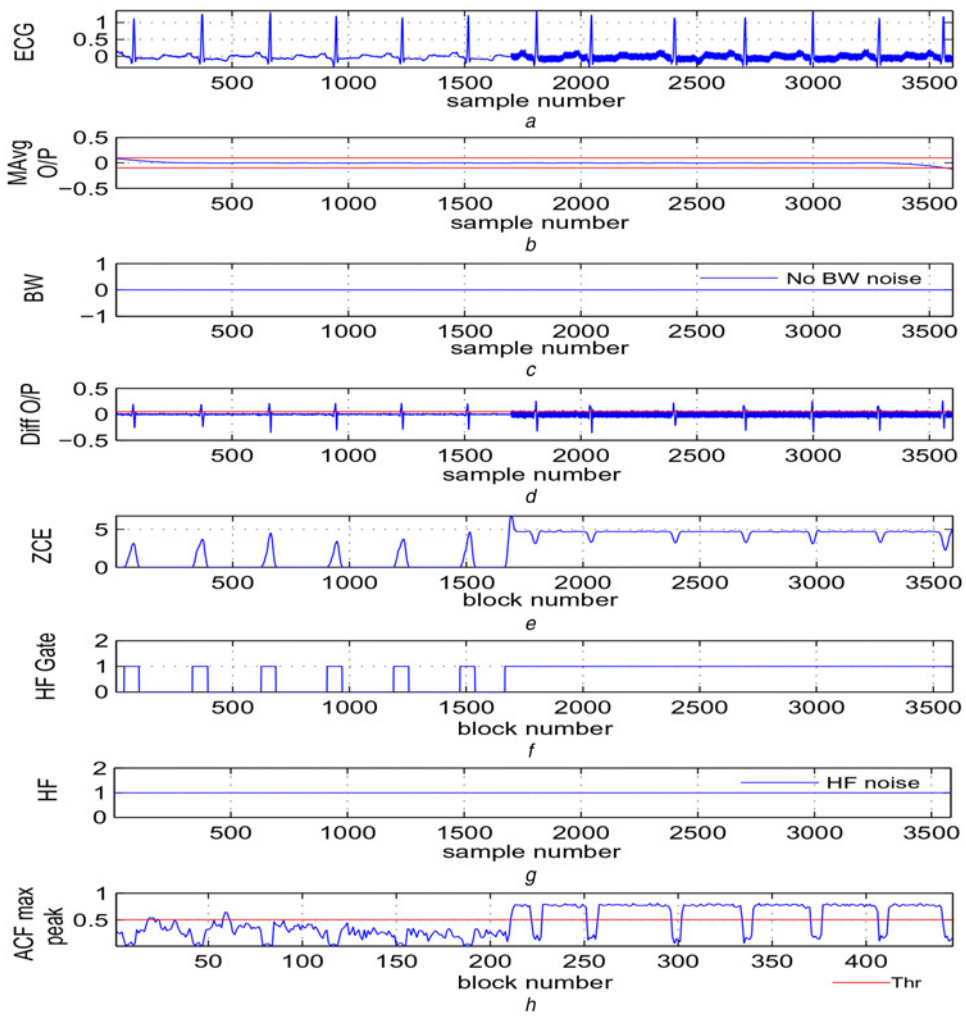

Fig. 3 *Noise detection and identification step*
a ECG with synthetically added PLI for half portion of segment taken from an MITBIHA record 100
b BW detection using MAA thresholding
c BW decision
d Difference operation output and MAA thresholding
e ZC envelope for detection of MA/PLI
f ZC thresholding for detection of MA
g MA decision
h ACF feature thresholding for detection of PLI

proposed noise detection and identification algorithm is summarised as

Step 1: In this step, low-frequency (LF) BW signal from ECG signal is extracted by using a moving average filter. The length of the moving average filter is chosen empirically such that it can capture the frequency component <1 Hz. In this Letter, the length of filter is chosen as 360. Based on the acceptable amplitude value of BW, an MAA of the extracted LF is compared with a predefined threshold of 0.05 mV for detecting the presence of BW. The acceptable amplitude value is decided such that it does not distort the minimum amplitude of P-wave. Typically, minimum amplitude of P-wave is 0.05 mV [17]. If the presence of BW is detected, the input signal is further processed for removal of BW component from an ECG signal using sparse signal decomposition algorithm.
Step 2: A first-order forward difference operation is performed for extracting the high-frequency (HF) noises including MA and PLI, which is implemented as

$$d[n] = \bar{x}[n] - \bar{x}[n-1], \quad n = 0, 1, 2, \ldots, N-1. \tag{1}$$

where $\bar{x}[n]$ is the normalised residual signal after subtracting the BW from $x[n]$ and N is the length of ECG signal. Since the HF signal $d[n]$ contains the HF portions of the QRS complexes, the HF signal is segmented into blocks with block size of 50 ms and block shift of one sample. Then, a number of zerocrossing (NZC) is computed for distinguishing the blocks containing QRS complex portion and noisy blocks. The overlapping blocking processing step is implemented as

$$d_l[n] = d[l+n], \quad n = 1, 2, \ldots, P \tag{2}$$

where $l = 0, 1, \ldots, N-P-1$. $d_l[n]$ is the lth block and P represents the block size. Then, the NZC is computed as

$$Z[l] = \begin{cases} \text{NZC}_l, & \text{if } \max(|d_l[n]|) > \gamma_2 \\ 0, & \text{otherwise} \end{cases} \tag{3}$$

where NZC_l is the NZCs for lth block which is computed as

$$\text{NZC}_l(m) = \frac{1}{2N+1} \sum_{n=-N}^{N} |\text{sgn}[d_l[n]] - \text{sgn}[d_l[n-1]]|. \tag{4}$$

doi: 10.1049/htl.2016.0077

The value of γ_2 is chosen based on the acceptable level of HF noise that can be used for reliable measurements of clinical parameters. Again, this acceptable level is decided based on typical minimum amplitude of P-wave. From the results, it is noted that the NZC for the noisy block is much higher than the block containing QRS complex. Therefore, we use zerocrossing (ZC) feature with duration threshold of 350 ms for discriminating the HF noise segments from the segments with localised QRS complex. By using the amplitude and duration criteria, the ECG segment is detected as noisy ECG signal. After detecting the presence of HF noise, the structured PLI is distinguished from the MA and instrument noise by using the ACF features. In this work, ACF features are computed by dividing the $d[n]$ into overlapping blocks of 100 ms with shift of 20% of the block

$$v_m[n] = d[0.2Pm + n], \quad n = 1, 2, \ldots, P \tag{5}$$

where $m = 0, 1, \ldots, M$, and $M = \lfloor \frac{N}{P} \rfloor$. Then, ACF sequence for each block $v_m(n)$ can be computed as

$$\phi_m(\tau) = \frac{1}{\mathrm{Q}} \sum_{n=0}^{\mathrm{Q}-1} v_m[n] v_m[n+\tau] \tag{6}$$

where $\phi_m(\tau)$ is the autocorrelation sequence for $v_m[n]$ and τ is the autocorrelation lag. Then, maximum of ACF with respect to first negative ZC point is found for each of the blocks. It is noted that the PLI and MA blocks are having maximum ACF values of >0.5 and <0.5, respectively. The feature extraction and detection results are shown in Figs. 2 and 3. Results demonstrate the effectiveness of the features for detecting and identifying the ECG noises. Based on the type of ECG noise identified, the representation dictionary learning is done for removal of identified noise(s) from the ECG signal. The noise detection and noise-aware dictionary learning can reduce the overall computational load of the ECG signal enhancement framework.

2.2. Noise-aware dictionary-learning-based algorithms: We present a generalised ECG signal enhancement framework based on the sparse signal decomposition on noise-aware learned dictionaries. For detailed discussion about the sparse signal decomposition, reader can refer our earlier reported work in [18]. An ECG signal $x[n]$, $n = 1, 2, \ldots, N$ is composed of time-localised and frequency-localised waveforms which can be represented on mixed dictionaries as

$$\boldsymbol{x} = \boldsymbol{\Phi}\rho = \sum_{i=1}^{N} \rho_i \phi_i, \tag{7}$$

where $\boldsymbol{\Phi} \in \mathbb{R}^{N \times M}$ (where $N < M$) is the mixed dictionary and $\rho = [\rho_1, \rho_2, \ldots, \rho_M]$ represents the sparse coefficient vector. The over-complete dictionary is constructed by analysing temporal-spectral information of local waves of the ECG signal. The frequency-localised components such as the LF components of ECG waves, the BW and PLI can be effectively modelled using sinusoids. The high-slope components of QRS complex and HF noises can be effectively modelled by impulses. Therefore, the representation dictionary is constructed as

$$\boldsymbol{\Phi} = [\boldsymbol{\Phi}_{\mathrm{B}} | \boldsymbol{\Phi}_{\mathrm{PT}} | \boldsymbol{\Phi}_{\mathrm{QRS}} | \boldsymbol{\Phi}_{\mathrm{D}} | \boldsymbol{\Phi}_{\mathrm{P}}], \tag{8}$$

where N denotes the length of ECG signal and M denotes the number of elementary waveforms. $\boldsymbol{\Phi}_{\mathrm{B}}$, $\boldsymbol{\Phi}_{\mathrm{PT}}$, $\boldsymbol{\Phi}_{\mathrm{QRS}}$, $\boldsymbol{\Phi}_{\mathrm{D}}$, and $\boldsymbol{\Phi}_{\mathrm{P}}$ consist of elementary waveforms to capture BW, P/T wave, wide portions of QRS complexes, spiky coefficients (contain HF component of QRS complex and HF noises), and PLI, respectively. To capture time-localised HF component of QRS complex and HF noises, $\boldsymbol{\Phi}_{\mathrm{D}} \in \mathbb{R}^{N \times N}$ is chosen as identity matrix. $\boldsymbol{\Phi}_{\mathrm{B}}$, $\boldsymbol{\Phi}_{\mathrm{PT}}$, $\boldsymbol{\Phi}_{\mathrm{QRS}}$, and $\boldsymbol{\Phi}_{\mathrm{P}}$ contain discrete sine and cosine basis vectors for the respective frequency range chosen from the $N \times N$ matrices $\boldsymbol{S}$ and $\boldsymbol{C}$. The atoms of $\boldsymbol{S}$ and $\boldsymbol{C}$ are given by

$$[\boldsymbol{S}]_{ij} = \sqrt{\frac{2}{N}} \left[a_i \sin\left(\frac{\pi(2j+1)(i+1)}{2N} \right) \right] \tag{9}$$

where $a_i = 1/\sqrt{2}$ for $i = N-1$, otherwise $a_i = 1$ and $i, j = 0, 1, 2, \ldots, N-1$.

$$[\boldsymbol{C}]_{ij} = \sqrt{\frac{2}{N}} \left[a_i \cos\left(\frac{\pi(2j+1)i}{2N} \right) \right] \tag{10}$$

where $a_i = 1/\sqrt{2}$ for $i = 0$, otherwise $a_i = 1$ and $i, j = 0, 1, 2, \ldots, N-1$. Both sine and cosine dictionaries are used together to avoid discontinuities at the block boundaries. Then the chosen dictionaries can be written as

$$\boldsymbol{\Phi} = [\boldsymbol{\Phi}^{\mathrm{C}}_{\mathrm{B}} | \boldsymbol{\Phi}^{\mathrm{S}}_{\mathrm{B}} | \boldsymbol{\Phi}^{\mathrm{C}}_{\mathrm{PT}} | \boldsymbol{\Phi}^{\mathrm{S}}_{\mathrm{PT}} | \boldsymbol{\Phi}^{\mathrm{C}}_{\mathrm{QRS}} | \boldsymbol{\Phi}^{\mathrm{S}}_{\mathrm{QRS}} | \boldsymbol{\Phi}^{\mathrm{C}}_{\mathrm{P}} | \boldsymbol{\Phi}^{\mathrm{S}}_{\mathrm{P}} | \boldsymbol{\Phi}_{\mathrm{D}}], \tag{11}$$

where $\boldsymbol{\Phi}^{\mathrm{C}}$ and $\boldsymbol{\Phi}^{\mathrm{S}}$ contain sinusoidal basis vectors chosen from cosine and sine dictionaries, respectively, as in (9) and (10). The frequencies of BW and PLI noises range between 0 and 0.8 Hz (upto 1 Hz during stress test) and 57–63 or 47–53 Hz, respectively [11]. However, most of the energy of ECG local P/T wave and wide QRS complex reside <1–5 and 5–20 Hz, respectively [11]. Based on aforementioned frequency information, dictionary learning for dictionaries $\boldsymbol{\Phi}_{\mathrm{B}}$, $\boldsymbol{\Phi}_{\mathrm{PT}}$, $\boldsymbol{\Phi}_{\mathrm{QRS}}$, and $\boldsymbol{\Phi}_{\mathrm{P}}$ is performed using sinusoidal elementary basis vectors of frequency ranges 0–1, 1–2, 2–20, and 47–53 Hz, respectively. The respective basis vectors for the frequency f will be the kth columns of $\boldsymbol{S}$ and $\boldsymbol{C}$ where, $k = \lfloor \frac{2Nf}{f_{\mathrm{s}}} \rfloor$ (f_{s} is the sampling rate). Then, the sparse coefficients for the respective dictionary can be

Table 1 Computational complexity analysis of the proposed method

Noise type	Dictionary [$\boldsymbol{\Phi}$]	Dictionary size	Comput. time, s	Pcg Iter.
BW	$[\boldsymbol{\Phi}_{\mathrm{B}}]$	$N \times 40$	0.29	43
PLI	$[\boldsymbol{\Phi}_{\mathrm{P}}]$	$N \times 240$	0.29	7
BW + PLI	$[\boldsymbol{\Phi}_{\mathrm{B}} \vert \boldsymbol{\Phi}_{\mathrm{P}}]$	$N \times 280$	0.37	20
MA	$[\boldsymbol{\Phi}_{\mathrm{PT}} \vert \boldsymbol{\Phi}_{\mathrm{QRS}} \vert \boldsymbol{\Phi}_{\mathrm{D}} \vert \boldsymbol{\Phi}_{\mathrm{P}}]$	$N \times (N + 1000)$	1.72	143
MA + PLI	$[\boldsymbol{\Phi}_{\mathrm{PT}} \vert \boldsymbol{\Phi}_{\mathrm{QRS}} \vert \boldsymbol{\Phi}_{\mathrm{D}} \vert \boldsymbol{\Phi}_{\mathrm{P}}]$	$N \times (N + 1000)$	1.81	158
MA + BW	$[\boldsymbol{\Phi}_{\mathrm{B}} \vert \boldsymbol{\Phi}_{\mathrm{PT}} \vert \boldsymbol{\Phi}_{\mathrm{QRS}} \vert \boldsymbol{\Phi}_{\mathrm{D}} \vert \boldsymbol{\Phi}_{\mathrm{P}}]$	$N \times (N + 1040)$	1.75	143
BW + MA + PLI	$[\boldsymbol{\Phi}_{\mathrm{B}} \vert \boldsymbol{\Phi}_{\mathrm{PT}} \vert \boldsymbol{\Phi}_{\mathrm{QRS}} \vert \boldsymbol{\Phi}_{\mathrm{D}} \vert \boldsymbol{\Phi}_{\mathrm{P}}]$	$N \times (N + 1040)$	1.90	165
Conventional	$[\boldsymbol{C} \vert \boldsymbol{S} \vert \boldsymbol{\Phi}_{\mathrm{D}}]$	$N \times 3N$	2.88	111

PCG Iter, preconditioned conjugate gradient iteration [19]

Table 2 Computational complexity analysis of existing methods

Noise type	Comput. time, s
Wavelet [15]	0.117
EMD + MM [14]	4.64
EMD [9]	0.966
EMD + wavelet [12]	0.969
DFT [20]	7.29×10^{-4}
Adaptive filter [20]	0.039
Notch [20]	0.0145

estimated by solving l_1 – norm convex optimisation [19]

$$\hat{\rho} = \arg\min . \|\boldsymbol{\Phi}\rho - \boldsymbol{x}\|_2^2 + \lambda\|\rho\|_1, \tag{12}$$

where λ regulates the reconstruction fidelity $\|\boldsymbol{\Phi}\rho - \boldsymbol{x}\|_2^2$ and sparsity term $\|\rho\|_1$. Here, the value of λ is taken 0.1 to suppress the low noisy peaks. $\hat{\rho}$ constitutes the reconstructed sparse coefficients corresponding to $\boldsymbol{\Phi}_{\mathrm{B}}$, $\boldsymbol{\Phi}_{\mathrm{PT}}$, $\boldsymbol{\Phi}_{\mathrm{QRS}}$, $\boldsymbol{\Phi}_{\mathrm{D}}$, and $\boldsymbol{\Phi}_{\mathrm{P}}$, respectively. Then the reconstructed ECG signal can be denoted as

$$\begin{aligned} \hat{\boldsymbol{x}} &\simeq \boldsymbol{\Phi}\hat{\rho} = [\boldsymbol{\Phi}_{\mathrm{B}}|\boldsymbol{\Phi}_{\mathrm{PT}}|\boldsymbol{\Phi}_{\mathrm{QRS}}|\boldsymbol{\Phi}_{\mathrm{D}}|\boldsymbol{\Phi}_{\mathrm{P}}][\hat{\rho}_{\mathrm{B}}|\hat{\rho}_{\mathrm{PT}}|\hat{\rho}_{\mathrm{QRS}}|\hat{\rho}_{\mathrm{D}}|\hat{\rho}_{\mathrm{P}}] \\ \hat{\boldsymbol{x}} &= \boldsymbol{\Phi}_{\mathrm{B}}\hat{\rho}_{\mathrm{B}} + \boldsymbol{\Phi}_{\mathrm{PT}}\hat{\rho}_{\mathrm{PT}} + \boldsymbol{\Phi}_{\mathrm{QRS}}\hat{\rho}_{\mathrm{QRS}} + \boldsymbol{\Phi}_{\mathrm{D}}\hat{\rho}_{\mathrm{D}} + \boldsymbol{\Phi}_{\mathrm{P}}\hat{\rho}_{\mathrm{P}} \end{aligned} \tag{13}$$

Finally, $\hat{\boldsymbol{x}}$ can be written as

$$\hat{\boldsymbol{x}} \simeq \hat{\boldsymbol{x}}_{\mathrm{B}} + \hat{\boldsymbol{x}}_{\mathrm{PT}} + \hat{\boldsymbol{x}}_{\mathrm{QRS}} + \hat{\boldsymbol{x}}_{\mathrm{D}} + \hat{\boldsymbol{x}}_{\mathrm{P}}, \tag{14}$$

where $\hat{\boldsymbol{x}}_{\mathrm{B}}$, $\hat{\boldsymbol{x}}_{\mathrm{PT}}$, $\hat{\boldsymbol{x}}_{\mathrm{QRS}}$, $\hat{\boldsymbol{x}}_{\mathrm{D}}$, and $\hat{\boldsymbol{x}}_{\mathrm{P}}$ are reconstructed BW signal, local P/T wave signal, wide QRS complex, HF QRS complex and other HF noises (detail signal), and PLI signal, respectively. In this Letter, we process 10 s segment of ECG and thus N is equal to $10f_{\mathrm{s}}$ number of samples. For example, in the presence of only BW noise, the dictionary can be chosen as $\boldsymbol{\Phi} = [\boldsymbol{\Phi}_{\mathrm{B}}^{\mathrm{C}}|\boldsymbol{\Phi}_{\mathrm{B}}^{\mathrm{S}}]_{N\times 2\lfloor\frac{2N}{f_{\mathrm{s}}}\rfloor} = [\boldsymbol{\Phi}_{\mathrm{B}}^{\mathrm{C}}|\boldsymbol{\Phi}_{\mathrm{B}}^{\mathrm{S}}]_{N\times 40}$ (by substituting $N = 10f_{\mathrm{s}}$). Similarly, the dictionaries $\boldsymbol{\Phi} = [\boldsymbol{\Phi}_{\mathrm{P}}^{\mathrm{C}}|\boldsymbol{\Phi}_{\mathrm{P}}^{\mathrm{S}}]_{N\times 240}$ (for 47–53 Hz) and $\boldsymbol{\Phi} = [\boldsymbol{\Phi}_{\mathrm{B}}^{\mathrm{C}}|\boldsymbol{\Phi}_{\mathrm{B}}^{\mathrm{S}}|\boldsymbol{\Phi}_{\mathrm{P}}^{\mathrm{C}}|\boldsymbol{\Phi}_{\mathrm{P}}^{\mathrm{S}}]_{N\times 280}$ are chosen in the presence of only PLI and BW + PLI, respectively. For removing the MA or MA + PLI, the dictionary $\boldsymbol{\Phi}$ is chosen as in (8) except $\boldsymbol{\Phi}_{\mathrm{B}}$. In the presence of all ECG noises including BW, MA, and PLI, a complete dictionary $\boldsymbol{\Phi} \in \mathbb{R}^{N\times M}$ (as in (8)) is used for ECG signal enhancement, where M is the total number of columns, i.e. $M = 40 + 40 + 720 + N + 240$. The proposed generalised ECG enhancement framework using noise-aware dictionary learning and sparse signal decomposition algorithms is summarised in Algorithm 1 for different kinds of noises. The computational load using noise-aware dictionary learning and computational load of existing de-noising methods are summarised in Tables 1 and 2. Evaluation results show that the overall computational load can be reduced by choosing a representation dictionary with suitable number of elementary waveforms based on the noise(s) to be removed from the ECG signal. The ECG denoising results are shown in Figs. 4 and 5. Results demonstrate the effectiveness of the proposed framework in simultaneous removal of combined noises from ECG signal. From our results, it is further noted that the QRS detection is not required in case of BW and/or PLI removal but it is required for MA removal meanwhile preserving the QRS complexes.

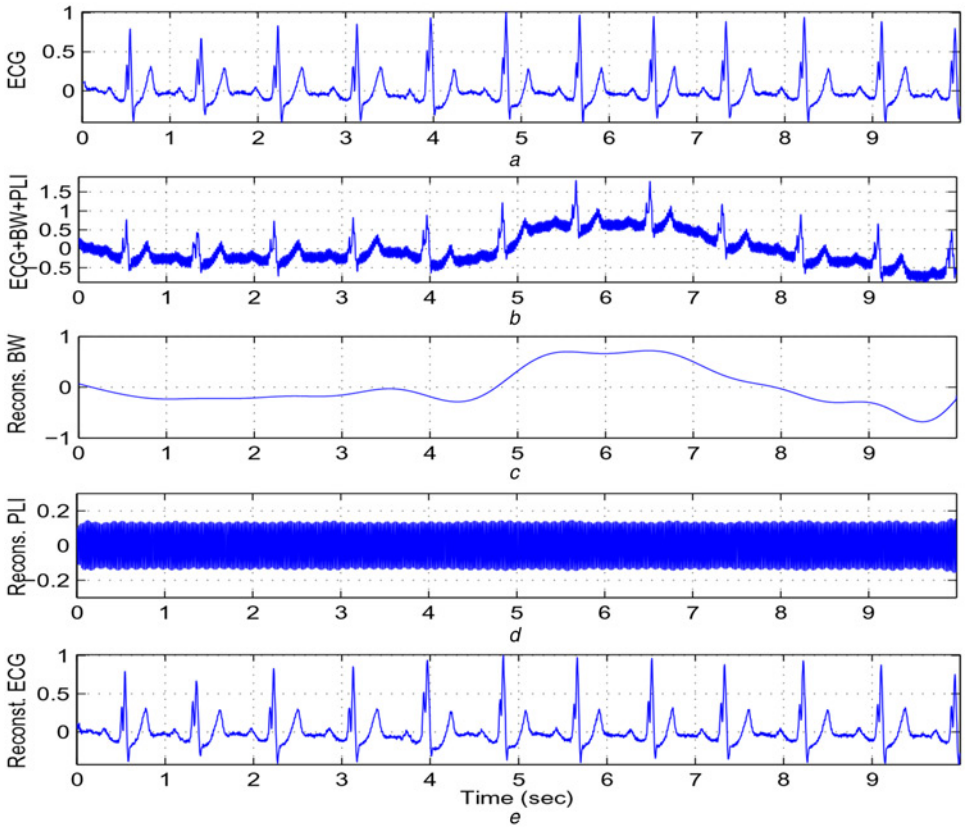

Fig. 4 *Effectiveness of the proposed framework in simultaneously removal BW and PLI*
a ECG signal taken from MITBIHA database record 111
b ECG signal with synthetically added BW and PLI noises
c Extracted BW signal
d Extracted PLI signal
e Reconstructed ECG signal after subtracting the BW and PLI signals from the noisy ECG signal

doi: 10.1049/htl.2016.0077

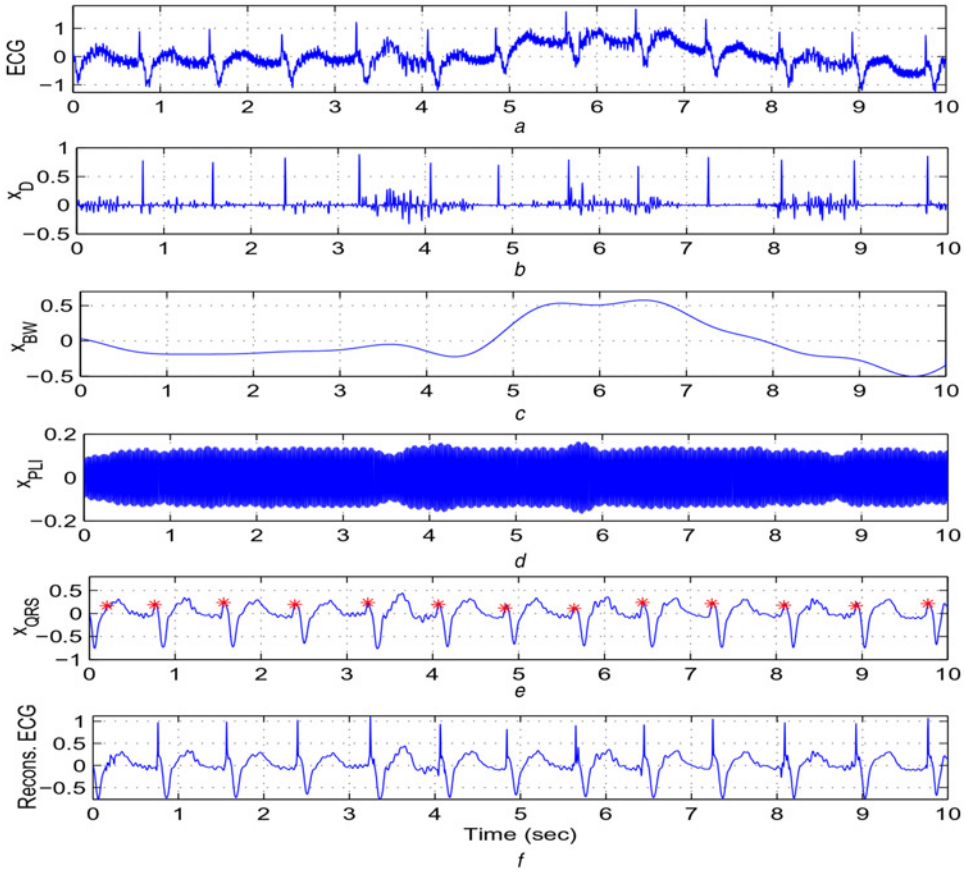

Fig. 5 *Effectiveness of the proposed framework in simultaneously removal of BW, PLI and MA (synthetically added)*
a ECG signal taken from MITBIHA record 104
b Extracted MA components
c Extracted BW signal
d Extracted PLI signal
e Identified R-peaks in QRS signal
f Reconstructed ECG after removal of the BW, PLI and MA signals

Algorithm 1: Generalised ECG enhancement framework using noise-aware dictionary learning and sparse signal decomposition
BW removal algorithm: If Noise type ←BW

- Obtain BW dictionary $\mathbf{\Phi}_B$.
- Perform sparse signal decomposition on $\mathbf{\Phi}_B$.
- Estimate the BW signal $\hat{\boldsymbol{x}}_B$.

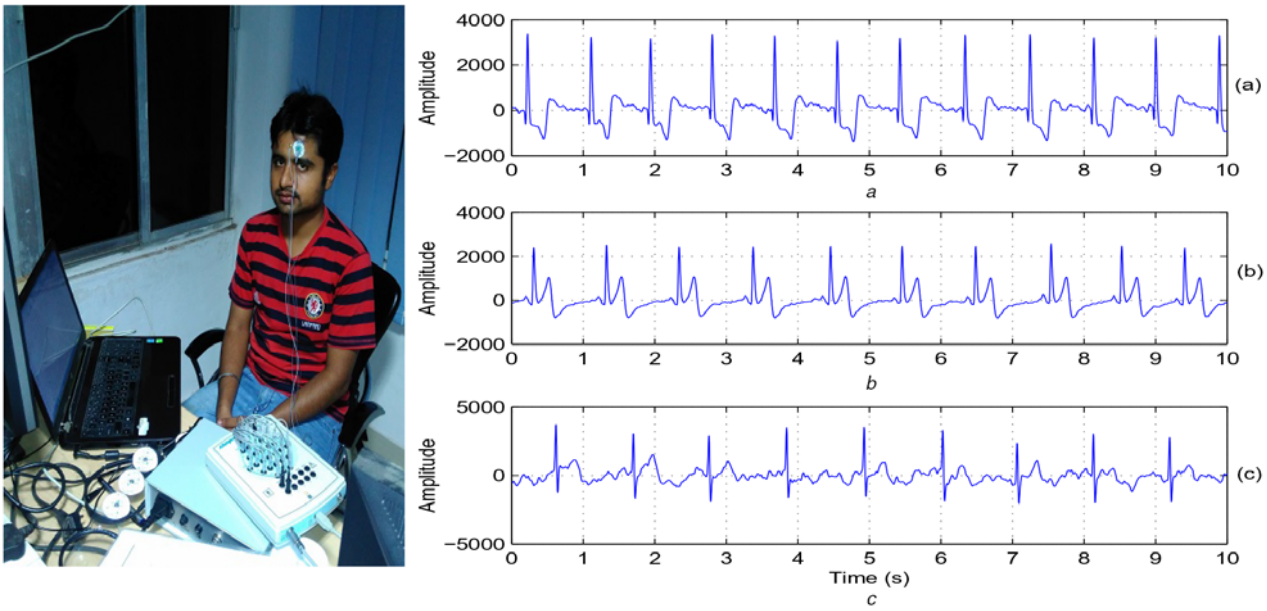

Fig. 6 *Experimental set-up and acquired ECG signals*

Table 3 Classification results of the proposed SQA method

Database	Noise	TS	TP	FP	FN	Se, %	+*P*, %	Acc, %
MITBIHA (Fs = 360 Hz, 11 bit resol.)	clean	1340	1340	16	0	100.00	98.82	98.82
	BW	1700	1681	11	19	98.88	99.35	98.25
	MA	2170	2148	8	22	98.99	99.63	98.62
	PLI	1770	1762	0	8	99.55	100.00	99.55
	BW + MA	2180	2159	15	21	99.04	99.31	98.36
	BW + PLI	1470	1449	9	21	98.57	99.38	97.97
	total	10,630	10,539	59	91	99.17	99.42	98.59

Fs: sampling frequency; resol.: resolution; TS: total segments; TP: true positive; FP: false positive; FN: false negative Se: sensitivity; +P: positive predictivity; Acc: accuracy

- Subtract estimated BW signal $\hat{\boldsymbol{x}}_{\mathrm{B}}$ from the ECG signal $\boldsymbol{x}$ for BW removal, i.e. $\tilde{\boldsymbol{x}} = \boldsymbol{x} - \hat{\boldsymbol{x}}_{\mathrm{B}}$; $\tilde{\boldsymbol{x}} \rightarrow$ denoised signal.

PLI removal algorithm: If Noise type ←PLI

- Obtain PLI dictionary $\boldsymbol{\Phi}_{\mathrm{P}}$.
- Perform sparse signal decomposition on $\boldsymbol{\Phi}_{\mathrm{P}}$.
- Estimate the PLI signal $\hat{\boldsymbol{x}}_{\mathrm{P}}$.
- Subtract estimated PLI signal $\hat{\boldsymbol{x}}_{\mathrm{P}}$ from the ECG signal $\boldsymbol{x}$ for PLI removal, i.e. $\tilde{\boldsymbol{x}} = \boldsymbol{x} - \hat{\boldsymbol{x}}_{\mathrm{P}}$; $\tilde{\boldsymbol{x}} \rightarrow$ denoised signal.

BW + PLI removal algorithm: If Noise type ← BW + PLI

- Obtain combined BW and PLI dictionaries $[\boldsymbol{\Phi}_{\mathrm{B}}|\boldsymbol{\Phi}_{\mathrm{P}}]$.
- Perform sparse signal decomposition on $[\boldsymbol{\Phi}_{\mathrm{B}}|\boldsymbol{\Phi}_{\mathrm{P}}]$.
- Estimate the BW signal $\hat{\boldsymbol{x}}_{\mathrm{B}}$ and the PLI signal $\hat{\boldsymbol{x}}_{\mathrm{P}}$.
- Subtract estimated BW and PLI signal from the ECG signal x for both BW and PLI removal, i.e. $\tilde{\boldsymbol{x}} = \boldsymbol{x} - \hat{\boldsymbol{x}}_{\mathrm{B}} - \hat{\boldsymbol{x}}_{\mathrm{P}}$; $\tilde{\boldsymbol{x}} \rightarrow$ denoised signal.

MA/MA + PLI removal algorithm: If Noise type ← MA/MA + PLI

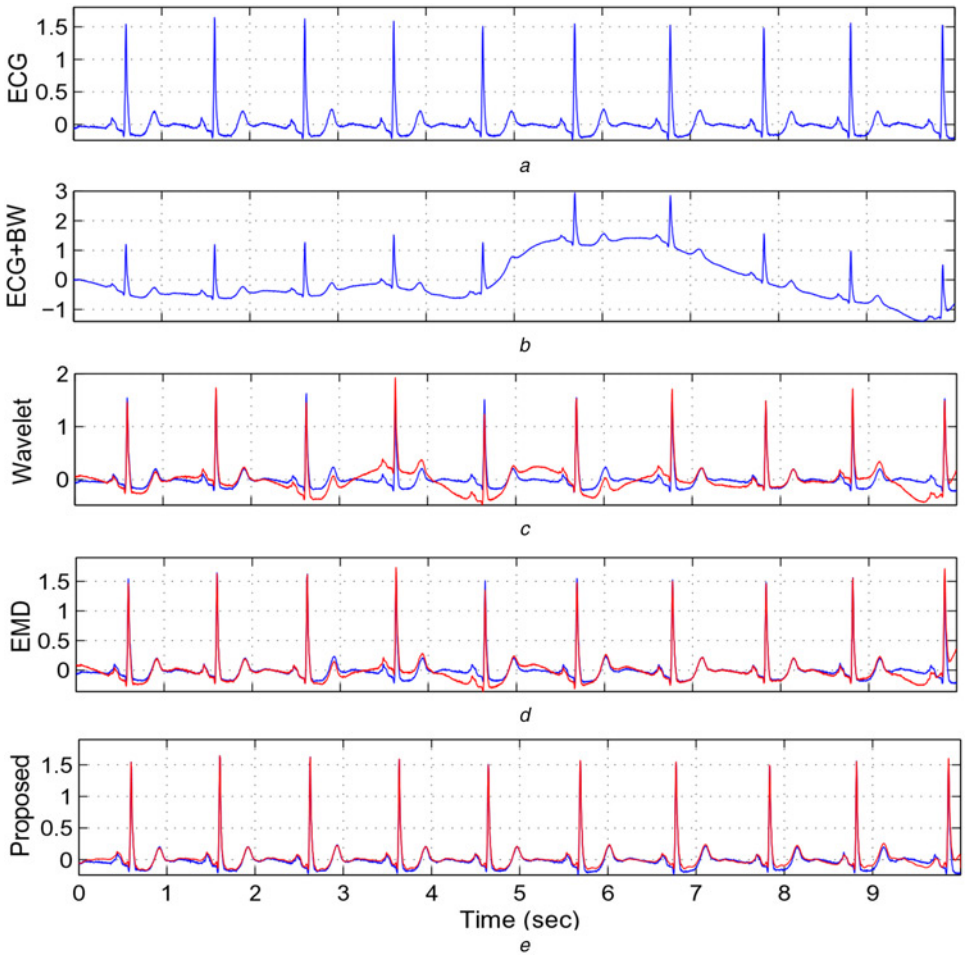

Fig. 7 *Performance of BW removal methods*
a Original ECG signal taken from MITBIHA record 101
b ECG corrupted with BW
c Wavelet-based method [15]
d EMD-based method [14]
e Proposed framework

doi: 10.1049/htl.2016.0077

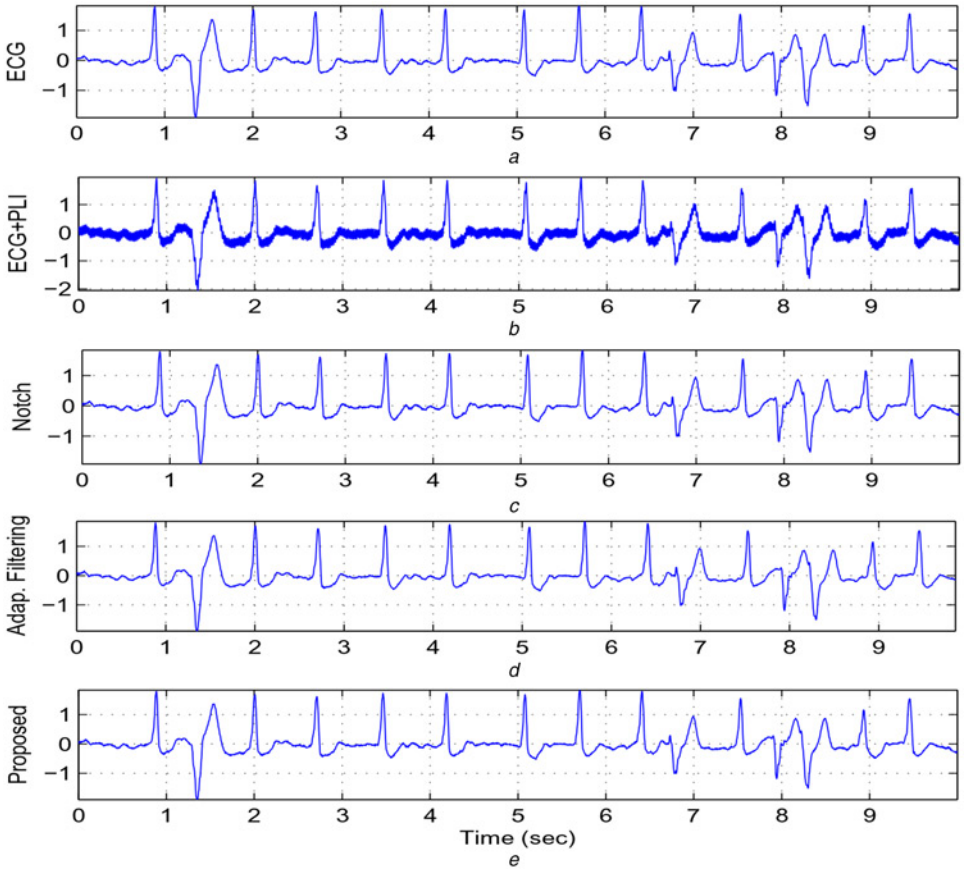

Fig. 8 *Performance of PLI removal methods*
a Original ECG taken from an MITBIHA record 203
b ECG signal plus PLI
c Notch filtering method [20]
d Adaptive filtering method [20]
e Proposed framework

- Obtain an over-complete dictionary of ECG, MA, and PLI noise $[\boldsymbol{\Phi}_{PT}|\boldsymbol{\Phi}_{QRS}|\boldsymbol{\Phi}_{D}|\boldsymbol{\Phi}_{P}]$.
- Perform sparse signal decomposition on the constructed over-complete dictionary.
- Estimate the PLI signal $\hat{\boldsymbol{x}}_{P}$, P/T wave $\hat{\boldsymbol{x}}_{P/T}$, QRS feature signal $\hat{\boldsymbol{x}}_{QRS}$, and detail signal or HF component of QRS complex $\hat{\boldsymbol{x}}_{D}$.
- Apply R-peak detection on QRS feature signal $\hat{\boldsymbol{x}}_{QRS}$.
- Extract HF portion of QRS complex from the $\hat{\boldsymbol{x}}_{D}$ within the block of block size (L) of 100 ms centred at the identified R-peak instants (let $n_1, n_2, \ldots, n_R$).

$$\mathrm{QRS}_{HF} = \begin{cases} \hat{\boldsymbol{x}}_{D}, & \text{for } n_i - L/2 \le n \le n_i + L/2 \\ 0, & \text{Otherwise} \end{cases}$$

$\tilde{\boldsymbol{x}} = \hat{\boldsymbol{x}}_{QRS} + \hat{\boldsymbol{x}}_{P/T} + \mathrm{QRS}_{HF}$; $\tilde{\boldsymbol{x}} \rightarrow$ denoised signal.

BW + MA/BW + MA + PLI removal algorithm: If Noise type ← BW + MA/BW + MA + PLI

- Obtain an over-complete dictionary of ECG, BW, MA, and PLI noise $[\boldsymbol{\Phi}_{B}|\boldsymbol{\Phi}_{PT}|\boldsymbol{\Phi}_{QRS}|\boldsymbol{\Phi}_{D}|\boldsymbol{\Phi}_{P}]$.
- Perform sparse signal decomposition on the constructed over-complete dictionary.
- Estimate the BW signal $\hat{\boldsymbol{x}}_{B}$, PLI signal $\hat{\boldsymbol{x}}_{P}$, P/T wave $\hat{\boldsymbol{x}}_{P/T}$, QRS feature signal $\hat{\boldsymbol{x}}_{QRS}$, and detail signal or HF component of QRS complex $\hat{\boldsymbol{x}}_{D}$.
- Apply R-peak detection on QRS feature signal $\hat{\boldsymbol{x}}_{QRS}$.
- Extract HF portion of QRS complex from the $\hat{\boldsymbol{x}}_{D}$ within the block of block size (L) of 100 ms centred at the identified R-peak instants (let $n_1, n_2, \ldots, n_R$).

$$\mathrm{QRS}_{HF} = \begin{cases} \hat{\boldsymbol{x}}_{D}, & \text{for } n_i - L/2 \le n \le n_i + L/2 \\ 0, & \text{Otherwise} \end{cases}$$

$\tilde{\boldsymbol{x}} = \hat{\boldsymbol{x}}_{QRS} + \hat{\boldsymbol{x}}_{P/T} + \mathrm{QRS}_{HF}$; $\tilde{\boldsymbol{x}} \rightarrow$ denoised signal.

3. Results and discussion: In this section, we evaluate the effectiveness of the proposed framework using noise-free and noisy ECG signals taken from a standard MIT-BIH arrhythmia (MITBIHA) database and real-time recorded ECG signals using Allengers medical system. The MITBIHA database consists of 48 two-channel ECG records recorded at sampling rate of 360 Hz and 11-bit resolution [21]. The performance of the denoising methods is evaluated using the real-time acquired ECG signals digitised with the sampling rate of 256 Hz and 16-bit resolution. The experimental set-up and acquired ECG signals are shown in Fig. 6.

In the first experiment, performance of the proposed noise detection and identification approach is evaluated in classifying single and combined ECG noises. The results of this experiment are summarised in Table 3. For performance evaluation, the noise-free and noisy ECG signals corrupted with various noises including BW, PLI, MA, BW + MA, BW + PLI, and BW + MA + PLI are taken from the MITBIHA database. Evaluation results show that the proposed noise detection and identification approach can achieve an average accuracy of 98.59% in classifying different kinds of single and combined ECG noises.

Table 4 Performance comparison for different ECG denosing methods in removal of BW and MA

Rec.	Performance evaluation for BW removal										Performance evaluation for MA removal									
	Wavelet [15]				EMD + MM [14]				Proposed method			EMD [9]			EMD + wavelet [12]				Proposed method		
	SNR	MAX	NCC	MOS	SNR	MAX	NCC	MOS	SNR	MAX	NCC	MOS	SNR	MAX	NCC	MOS	SNR	MAX	NCC	MOS	SNR	MAX	NCC	MOS
101	2.80	0.42	0.810	2.15	10.94	0.27	0.893	3.14	15.42	0.20	0.992	4.54	11.17	0.46	0.967	4.17	10.81	0.52	0.963	4.08	16.48	0.20	0.992	4.58
104	3.09	0.45	0.818	2.05	11.84	0.40	0.827	2.68	16.66	0.22	0.991	4.53	12.42	0.54	0.971	4.29	11.27	0.61	0.963	4.11	16.44	0.48	0.989	4.54
107	13.03	0.59	0.975	4.04	19.07	0.41	0.985	4.37	24.98	0.30	0.998	5.00	16.59	0.73	0.989	4.48	16.41	0.73	0.988	4.43	22.03	0.48	0.997	5.00
109	8.11	0.44	0.929	3.51	18.63	0.34	0.982	4.31	20.85	0.26	0.996	4.95	12.46	0.58	0.970	4.14	12.45	0.58	0.970	4.34	22.08	0.20	0.997	4.98
111	1.17	0.42	0.753	1.84	11.05	0.25	0.852	2.89	15.87	0.20	0.988	4.62	9.92	0.44	0.948	3.83	11.09	1.00	0.948	3.81	14.68	0.21	0.984	4.81
113	6.42	0.43	0.902	3.12	14.60	0.36	0.961	4.02	15.97	0.27	0.993	4.57	10.65	0.72	0.953	3.91	11.34	0.96	0.964	4.05	16.70	0.54	0.989	4.86
119	8.44	0.45	0.932	3.57	15.38	0.41	0.961	4.13	17.61	0.31	0.994	4.80	13.16	0.90	0.974	4.18	13.19	0.89	0.974	4.28	19.38	0.48	0.996	4.91
124	7.07	0.51	0.908	3.24	10.22	0.63	0.837	2.67	17.58	0.24	0.992	4.73	13.64	0.71	0.974	4.17	13.62	0.73	0.974	4.31	18.89	0.45	0.994	4.9
203	7.92	0.46	0.926	3.59	13.50	0.43	0.938	3.66	19.33	0.28	0.995	5.00	13.60	0.57	0.978	4.26	13.58	0.58	0.978	4.33	19.77	0.37	0.995	4.94
208	8.44	0.44	0.935	3.68	15.93	0.35	0.967	4.11	18.27	0.34	0.995	4.88	13.54	0.76	0.978	4.29	13.40	0.80	0.978	4.37	18.28	0.64	0.993	4.91
Sub.1	11.08	0.52	0.851	3.89	12.63	0.48	0.911	4.02	20.30	0.23	0.995	5.00	10.45	0.67	0.846	3.79	12.19	0.82	0.974	4.29	20.79	0.18	0.992	4.99
Sub.2	9.55	0.51	0.895	4.16	16.55	0.34	0.945	4.17	17.49	0.24	0.990	4.93	14.66	0.73	0.932	4.04	11.09	1.00	0.948	3.91	19.35	0.45	0.987	4.82
Avg.	7.26	0.47	0.886	3.24	14.20	0.39	0.922	3.68	18.36	0.26	0.993	4.80	12.69	0.65	0.957	4.13	12.53	0.77	0.968	4.19	18.74	0.39	0.992	4.85

In the second experiment, effectiveness of the sparse representation-based ECG noise removal algorithm using the noise-aware dictionary learning approach is investigated using a wide variety of noisy ECG signals. The reconstructed ECG signals are assessed using both subjective quality assessment test and objective quality assessment metrics. The objective quality metrics including the signal-to-noise ratio (SNR), maximum absolute error (MAX), and normalised cross correlation (NCC) are computed for the clean and reconstructed signals which are computed as $\mathrm{SNR} = 10\log_{10}\left[\sum_{n=1}^{N}(x[n]-\mu_0)^2 / \sum_{n=1}^{N}(x[n]-\tilde{x}[n])^2\right]$, $\mathrm{MAX}_i = \max_{n=1}^{N_{ci}}\{|x[n]-\tilde{x}[n]|\}$, and

$$\mathrm{NCC} = \frac{(1/N)\sum_{n=1}^{N}[x[n]-\mu_0]\sum_{n=1}^{N}[\tilde{x}[n]-\mu_r]}{\sqrt{(1/N)\sum_{n=1}^{N}[x[n]-\mu_0]}\sqrt{(1/N)\sum_{n=1}^{N}[\tilde{x}[n]-\mu_r]}}$$

where N_{ci} is the number of samples in ith cycle, and μ_0 and μ_r are mean of the original and reconstructed signal, respectively [22]. These objective distortion metrics quantify the global and local distortions in the reconstructed ECG signal. In subjective quality test, a mean opinion score (MOS) is computed based on the ratings (1-Very Bad, 2-Bad, 3-Good, 4-Very Good, and 5-Excellent) obtained for the reconstructed ECG signals [22].

For performance comparison, we implemented seven denoising methods such as wavelet [15], EMD [9], EMD + mathematical morphology (MM) [14], EMD + wavelet [12], adaptive filter [20], notch filter [20], and DFT filtering [20] in this work. The denoising results of the proposed framework and existing methods are shown in Figs. 7 and 8 for different types of noisy ECG signals. By visual inspection of local waves of the reconstructed signal, it is noted that the proposed ECG signal enhancement framework can effectively remove the noises and preserves morphological features of the local waves of ECG signal. In most MA removal methods, it is noted that the amplitude of the QRS complex is not preserved in the reconstructed ECG signal [11]. Results further show that MA is not completely removed from the ECG signal. By visual inspection of the denoising results, it is noted that most BW removal methods distort the low-frequency components of the ECG signal. For all types of ECG noises, the proposed framework results better noise-reduction capability without distorting the morphological features such as amplitude, duration, and shape of the local waves. Results of the objective quality test and subjective quality test are summarised in Tables 4–7.

For ECG signals taken from the record 101, 104, 107, 109, 111, 113, 119, 124, 203, and 208 including different kinds of beat morphologies such as normal, paced, premature ventricular contraction, left bundle branch block, right bundle branch block, and fusion beats, and sudden change in QRS amplitudes, irregular heart rates, sudden changes in morphologies and low-amplitude beats and the real-time ECG signals. For performance comparison, different kinds of ECG noise patterns are generated and added to the noise-free ECG signals [23]. From the results of BW removal methods, the proposed method achieves better NCC, SNR and MAX values for most test ECG signals when compared with the wavelet-based and EMD + MM-based methods. From results summarised in Table 4, the proposed MA removal method outperforms EMD and EMD + wavelet in terms of NCC, SNR, and MAX values. Table 5 demonstrates the effectiveness of the proposed method for the ECG signals taken from the record 102, 106, 109, 111, 118, 123, 203, 208, and the real-time ECG signals. Table 6 shows the performance of the methods for simultaneous removal of BW and PLI noises from ECG signals. The proposed method outperforms the DFT-based method in removal of BW plus PLI noise. From the quality assessment results summarised in Table 7, it is observed that the proposed method can achieve better noise reduction meanwhile preserving the morphological content for combined noise sources (BW + MA and BW + MA + PLI).

doi: 10.1049/htl.2016.0077

Table 5 Performance comparison for PLI removal

Rec.	Adaptive filter LMS [20]				Notch [20]				Proposed method			
	SNR	MAX	NCC	MOS	SNR	MAX	NCC	MOS	SNR	MAX	NCC	MOS
102	21.28	0.14	0.995	4.78	26.39	0.09	0.999	4.79	27.78	0.05	0.999	4.96
106	23.45	0.17	0.998	4.86	28.66	0.10	0.999	4.89	28.61	0.08	0.999	4.91
109	29.88	0.11	0.999	5.00	34.09	0.10	1.000	4.91	36.70	0.05	1.000	5.00
111	22.91	0.08	0.997	4.81	28.79	0.10	0.999	4.83	35.31	0.04	1.000	5.00
118	24.15	0.08	0.998	4.87	27.63	0.10	0.999	4.72	34.86	0.03	1.000	5.00
123	29.05	0.10	0.999	4.98	30.13	0.10	0.999	4.92	35.01	0.06	1.000	4.99
203	28.08	0.09	0.999	5.00	34.27	0.10	1.000	4.95	36.89	0.05	1.000	5.00
208	27.47	0.20	0.999	4.99	32.08	0.10	1.000	4.94	32.91	0.06	1.000	5.00
Sub.3	24.55	0.19	0.992	4.84	24.61	0.09	0.997	4.78	29.65	0.07	0.998	4.83
Sub.4	22.15	0.11	0.991	4.78	34.09	0.12	0.998	4.89	31.44	0.05	0.994	4.93
Avg.	25.30	0.13	0.997	4.89	30.07	0.10	0.999	4.86	32.92	0.05	0.999	4.96

Table 6 Performance comparison for BW + PLI removal

Rec.	DFT [20]				Proposed method			
	SNR	MAX	NCC	MOS	SNR	MAX	NCC	MOS
102	12.39	0.25	0.971	4.25	20.90	0.21	0.995	4.93
109	20.08	0.26	0.995	4.72	23.75	0.35	0.996	4.93
111	12.68	0.26	0.973	4.16	22.09	0.21	0.997	4.98
119	16.86	0.26	0.989	4.37	23.83	0.30	0.997	5.00
124	17.92	0.27	0.990	4.51	22.43	0.33	0.995	4.99
203	17.96	0.24	0.992	4.59	23.61	0.27	0.997	4.97
208	19.35	0.23	0.994	4.83	23.33	0.34	0.997	4.98
Sub.5	13.55	0.28	0.971	4.07	21.49	0.24	0.994	4.84
Sub.6	15.17	0.22	0.964	4.18	23.61	0.28	0.995	4.89
Avg.	16.22	0.25	0.982	4.41	22.78	0.28	0.996	4.95

Table 7 Performance of the proposed method for BW + MA and BW + MA + PLI removal

Rec.	For BW + MA removal				For BW + MA + PLI removal			
	SNR	MAX	NCC	MOS	SNR	MAX	NCC	MOS
101	13.18	0.33	0.979	4.14	13.13	0.34	0.978	4.19
104	13.26	0.54	0.976	4.11	13.37	0.50	0.977	4.15
109	18.46	0.31	0.993	4.69	18.40	0.32	0.993	4.82
119	16.28	0.50	0.989	4.57	16.25	0.50	0.989	4.41
124	16.05	0.49	0.987	4.52	16.03	0.50	0.987	4.59
203	16.94	0.41	0.990	4.81	16.93	0.41	0.990	4.67
208	15.23	0.93	0.985	4.78	15.12	0.91	0.984	4.41
Sub.7	15.54	0.44	0.991	4.62	14.37	0.64	0.964	4.64
Sub.8	16.44	0.38	0.993	4.45	15.12	0.87	0.983	4.48
Avg.	15.71	0.48	0.987	4.52	15.41	0.55	0.983	4.48

In the third experiment, the computational complexity analysis is performed by implementing the denoising methods on intel i5-4210U CPU @ 1.70 GHz-2.40 GHz with 4 GB of RAM and MATLAB software. The computational time for each of the denoising methods are shown in Tables 1 and 2. Although the computational time of the existing methods such as wavelet, EMD, EMD + wavelet, DFT, adaptive filter, notch filter, is lesser than the proposed framework, the existing methods had poor denoising performance in removal of single ECG noise. However, the proposed noise-aware dictionary-learning-based sparse representation can reduce the computational time when compared with the conventional sparse representation on over-complete mixed dictionaries. In the future directions, we further study the computational load by implementing the proposed framework on embedded processors.

4. Conclusion: This Letter presents a noise-aware dictionary-learning-based generalised ECG signal enhancement framework for automatically detecting and removal of single and combined noises such as BWs, power-line interference, muscle artefacts and their combinations. The proposed framework consists of three major steps: noise detection and identification, noise-aware dictionary learning, sparse signal decomposition and reconstruction algorithms. The proposed framework is evaluated on the noise-free and noisy ECG signals taken from the MIT-BIH arrhythmia database and the real-time acquired ECG signals. The quality assessment results show that the proposed framework outperforms existing DFT, wavelet, EMD, wavelet and EMD, EMD and MM, and adaptive filtering methods in automatically detecting and removing single and combined noises

simultaneously without distorting the morphological content of local waves of the ECG signal. Results further demonstrate that the proposed framework based on noise-aware dictionary-learning approach can significantly reduce computational load when compared with conventional sparse representation on over-complete mixed dictionaries.

5. Funding and declaration of interests: Conflict of interest: none declared.

6 References

[1] Sanei S., Lee T.K., Abolghasemi V.: 'A new adaptive line enhancer based on singular spectrum analysis', *IEEE Trans. Biomed. Eng.*, 2012, **59**, (2), pp. 428–434

[2] Roonizi E.K., Sassi R.: 'A signal decomposition model-based Bayesian framework for ECG components separation', *IEEE Trans. Signal Process.*, 2016, **64**, (3), pp. 665–674

[3] Vullings R., De Vries B., Bergmans J.W.: 'An adaptive Kalman filter for ECG signal enhancement', *IEEE Trans. Biomed. Eng.*, 2011, **58**, (4), pp. 1094–1103

[4] Yadav S.K., Sinha R., Bora P.K.: 'Electrocardiogram signal denoising using non-local wavelet transform domain filtering', *IET Signal Process.*, 2015, **9**, (1), pp. 88–96

[5] Gao J., Sultan H., Hu J., *ET AL.*: 'Denoising nonlinear time series by adaptive filtering and wavelet shrinkage: a comparison', *IEEE Signal Process. Lett.*, 2010, **17**, (3), pp. 237–240

[6] Hesar H., Mohebbi M.: 'ECG denoising using marginalized particle extended kalman filter with an automatic particle weighting strategy', *IEEE J. Biomed. Health Informatics*, 2016, accepted. doi: 10.1109/JBHI.2016.2582340

[7] Karagiannis A., Constantinou P.: 'Noise-assisted data processing with EMD in biomedical signals', *IEEE Trans. Inf. Technol. Biomed.*, 2011, **15**, (1), pp. 11–18

[8] Lahmiri S.: 'Comparative study of ECG signal denoising by wavelet thresholding in empirical and variational mode decomposition domains', *Healthcare Technol. Lett.*, 2014, **1**, (3), pp. 104–109

[9] Weng B., Blanco-Velasco M., Barner K.E.: 'ECG denoising based on the empirical mode decomposition'. 28th Int. Conf. IEEE EMBS, 2006, pp. 1–4

[10] Sameni R., Shamsollahi M.B., Jutten C., *ET AL.*: 'A nonlinear Bayesian filtering framework for ECG denoising', *IEEE Trans. Biomed. Eng.*, 2007, **54**, (12), pp. 2172–2185

[11] Satija U., Ramkumar B., Manikandan M.S.: 'A unified sparse signal decomposition and reconstruction framework for elimination of muscle artifacts from ECG signal'. IEEE ICASSP, 2016, pp. 779–783

[12] Kabir A., Shahnaz C.: 'Denoising of ECG signals based on noise reduction algorithms in EMD and wavelet domains', *Biomed. Sig. Process. Control*, 2012, **7**, (5), pp. 481–489

[13] Zivanovic M., González-Izal M.: 'Simultaneous powerline interference and baseline wander removal from ECG and EMG signals by sinusoidal modeling', *Med. Eng. Phys.*, 2013, **35**, (10), pp. 1431–1441

[14] Ji T.Y., Lu Z., Wu Q.H., *ET AL.*: 'Baseline normalization of ECG signals using empirical mode decomposition and mathematical morphology', *Electron. Lett.*, 2008, **44**, (2), pp. 82–83

[15] Zhang D.H.: 'Wavelet approach for ECG baseline wander correction and noise reduction'. Proc. 27th IEEE EMBS, 2005, pp. 1212–1215

[16] Leski J.M., Henzel N.: 'ECG baseline wander and power line interference reduction using nonlinear filter bank', *Signal Process.*, 2005, **85**, pp. 781–793

[17] Havmoller R., Carlson J., Holmqvist F., *ET AL.*: 'Age-related changes in P wave morphology in healthy subjects', *BMC Cardiovasc. Disord.*, 2007, **7**, (1), p. 22

[18] Manikandan M.S., Ramkumar B.: 'Straightforward and robust QRS detection algorithm for wearable cardiac monitor', *Healthcare Technol. Lett.*, 2014, **1**, (1), pp. 40–44

[19] Candes E.J., Romberg J., Tao T.: 'Robust uncertainty principles: exact signal reconstruction from highly incomplete frequency information', *IEEE Trans. Inf. Theory*, 2006, **52**, pp. 489–509

[20] Rangayyan R.M.: 'Biomedical signal analysis: a case study approach' (Wiley, 2009)

[21] Moody G.B., Mark R.G.: 'The impact of the MIT-BIH Arrhythmia Database', *IEEE Eng. Med. Biol.*, 2001, **20**, (3), pp. 45–50. http://physionet.org/physiobank/database/mitdb

[22] Manikandan M.S., Dandapat S.: 'Wavelet energy based diagnostic distortion measure for ECG', *Biomed. Sig. Process. Control*, 2007, **2**, (2), pp. 80–96

[23] McSharry P.E., Clifford G.D.: 'ECGSYN-waveform generator', http://www.physionet.org/physiotools/ecgsyn/